Oxygen-Generating Nanofiber Cell Scaffolds with Antimicrobial Properties

Junping Wang,[†] Yizhou Zhu,[†] Harinder K. Bawa,[†] Geoffrey Ng,[†] Yong Wu,[‡] Matthew Libera,[‡] H.C. van der Mei,[§] H.J. Busscher,[§] and Xiaojun Yu*[,†]

Department of Chemistry, Chemical Biology, and Biomedical Engineering, and Department of Chemical Engineering and Materials Science, Stevens Institute of Technology, Hoboken, New Jersey 07030, United States, and Department of Biomedical Engineering, University Medical Center Groningen and University of Groningen, Antonius Deusinglaan 1, 9713 AV Groningen, The Netherlands

ABSTRACT Many next-generation biomaterials will need the ability to not only promote healthy tissue integration but to simultaneously resist bacterial colonization and resulting biomaterials-associated infection. For this purpose, antimicrobial nanofibers of polycaprolactone (PCL) were fabricated by incorporating calcium peroxide. PCL nanofibers containing different ratios of calcium peroxide (1%, 5% and 10% (w/w)) with or without ascorbic acid were fabricated using an electrospinning technique. Antimicrobial evaluations confirmed the inhibitory properties of the nanofibers on the growth of *E. coli* and *S. epidemidis* because of a significant burst release of calcium peroxide from the nanofibers. Analysis of tissue cell response showed that despite an initial toxic effect over the first 24 h, after 4 days of culture, osteoblast viability and morphology were both healthy. These results demonstrate that oxygen-generating nanofibers can be designed and developed to provide a short-term peroxide-based antimicrobial response while still maintaining attractive tissue-integration properties.

KEYWORDS: antimicrobial • electrospinning • nanofibers • calcium peroxide • oxygen-generating • osteoblast

INTRODUCTION

More than one million cases of device-related infection occur each year in the United States (1). Such infections occur when opportunistic bacteria adhere to and colonize the surface of a biomedical device and infect the surrounding tissue. When the bacterial colonies develop into biofilms (2, 3), they become extremely resistant to antibiotic s (4), and resolution of the tissue infection usually requires that the device be removed. In the particular case of orthopedic implants, treatment of a device-related infection usually requires removal of the device, debridement of the infected bone and/or surrounding soft tissue, replacement of the implant, and extensive antibiotic therapy (5). Importantly, biomaterials-associated infection has emerged as one of the primary failure mechanisms of biomedical devices (6−9).

Numerous strategies have been investigated to prevent bacterial colonization and subsequent biofilm formation on the surfaces of synthetic implants. Implant surfaces can, for example, be modified to be either antiadhesive or colonization-resistant via physical-chemical methods, such as PEGylation, which blocks protein adsorption and microbial adhesion (10), or by the application of positively charged polymer coatings with antimicrobial properties (11). Although many in vitro studies have demonstrated the efficacy of such strategies, modified surfaces may become fouled by plasma proteins after long-term in vivo use, potentially invalidating the coating principle (12). At the same time, a surface that is nonadhesive to bacteria can be expected to also yield poor tissue integration (13). Antimicrobial agents such as gentamycin, vancomycin, or ciprofloxacin (14); biocides such as nitric oxide (15); and bleaching agents (16) and silver-based agents (17) have also been incorporated either into implant materials themselves or into coatings applied to an implant surface. Although these strategies are successful to a certain extent in some specific situations, they all have varying degrees of limitations for use. Novel strategies are still needed not only to resist bacterial colonization and the resulting biomaterials-associated infection but also to simultaneously promote healthy tissue integration.

Hydrogen peroxide (H_2O_2) is widely recognized as an effective biocide and, among other applications areas, is used extensively in oral health care products (18−20). Through the oxidation of proteins, oxygen radicals produced by hydrogen peroxide can effectively kill bacteria and prevent biofilm formation (21). Even at low concentrations, H_2O_2 can limit biofilm development by the inhibition of glycolysis and the repression of the biofilm regulator gene (22, 23) with minimal damage to surrounding host tissue. Particularly in orthopedics, the local application of H_2O_2 can be advantageous, because relatively high levels can be achieved around an implant without systemic toxicity (24). Kristensen et al., for example, showed a strong antifouling

* Corresponding author. E-mail: xyu@stevens.edu. Phone: 201-216-5256. Fax: 201-216-8306.

Received for review September 10, 2010 and accepted November 24, 2010

[†] Department of Chemistry, Chemical Biology, and Biomedical Engineering, Stevens Institute of Technology.

[‡] Department of Chemical Engineering and Materials Science, Stevens Institute of Technology.

[§] University Medical Center Groningen and University of Groningen.

DOI: 10.1021/am100862h

Table 1. Oxygen-Generating Nanofibers Fabrication Parameters

group	name	HFIP (mL)	polymer (g)	CP (g)	AC (g)	rate (mL/h)	needle distance to platform (cm)
1	PCL	0.5	0.4			0.18	15
2	PCL 1%CP	0.5	0.4	0.004		0.18	15
2	PCL 5%CP	0.5	0.4	0.02		0.25	18
3	PCL10%CP	0.5	0.4	0.04		0.5	18
5	PCL 1%CP 1%AC	0.5	0.4	0.004	0.004	0.18	15
6	PCL 5%CP 5%AC	0.5	0.4	0.02	0.02	0.25	18
7	PCL10%CP10%AC	0.5	0.4	0.04	0.04	0.5	18

effect of hydrogen peroxide produced by an enzymatic method (25).

Calcium hydroxide has also been reported to be able to kill bacteria (26). In dental applications, calcium hydroxide has been used as a root canal sealant with antimicrobial effects (27). It has also been reported that the additional use of oxidants with calcium hydroxide showed higher antibacterial efficacy against *Enterococcus faecalis* than using calcium hydroxide alone (28).

When reacted with water, calcium peroxide can produce hydrogen peroxides and calcium hydroxides (eq 1), and, to exploit this behavior, we have incorporated calcium peroxide as an oxygen-generating material into polymeric nanofibers. We speculate that loading calcium peroxide into polymeric nanofibers will impart antimicrobial properties while preserving their inherently strong ability of nanofibers to facilitate tissue regeneration. Moreover, ascorbic acid was incorporated as a cell protector (29) in order to alleviate potentially harmful oxidative stress on osteoblasts. Specifically, PCL nanofibers containing different concentrations of calcium peroxide (1, 5, and 10%) (w/w) with and without ascorbic acid were fabricated by electrospinning. The antibacterial susceptibility of the oxygen-generating nanofibers was evaluated by a colorimetric assay and a modified Kirby-Bauer test involving *Escherichia coli (E. coli)* and *Staphylococcus epidermidis (S. epidermidis)*. In addition, the cytotoxicity of the nanofibers to the human osteoblast cells was tested by the cell proliferation assay, and the morphological changes of the cells were also observed from confocal microscopy.

$$CaO_2 + 2H_2O \rightarrow Ca(OH)_2 + H_2O_2 \qquad (1)$$

EXPERIMENTAL SECTION

Materials. All solutions were prepared with distilled and deionized water. All the chemicals if not otherwise specified were obtained from Sigma Aldrich (St. Louis, MO).

Nanofiber Fabrication. PCL electrospun nanofibers were fabricated by electrospinning. Briefly, PCL (M_w = 80 kDa) was dissolved in hexafluoroisopropanol (HFIP) (Oakwood Products, Inc.). Calcium peroxide and L-ascorbic acid were then mixed at ratios listed in Table 1 within the PCL-HFIP solution by magnetic stirring overnight to form a homogeneous suspension. The mixture was delivered at a constant flow rate (KD Scientific syringe pump) to a metal capillary connected to a high-voltage power supply (Gamma High Voltage Research ES-30P, Ormond Beach, FL). By applying a high voltage (17−20 kV), nanofibers were electrospun from the needle into sheets on a silicon wafer (Ted Pella; 5 mm ×7 mm). The electrospun nanofiber sheets were placed into a vacuum desiccator to remove excess solvent. The parameters of seven experimental groups including the composition, the flow rate and the distance are listed in Table 1. Before initiating either an antimicrobial experiment or osteoblast cell experiment, nanofibers were sterilized by being exposed under UV light for 30 min.

Nanofiber Characterization. The morphology of electrospun nanofibers was observed with a Nikon 1500z stereo optical microscope and a scanning electron microscope (LEO 982 FEG-SEM). For the SEM observation, oxygen-generating nanofibers (PCL/10%CP and PCL10%CP/10%AC) were electrospun directly onto aluminum SEM stubs that were then mounted on the grounded collector plate of the electrospinning apparatus. Oxygen-generating nanofibers treated with deionized (DI) water were prepared by immersing the nanofibers from these two groups in DI water for 24 h and then drying them in a vacuum desiccator. Prior to SEM observation, both DI water-treated and nontreated samples were coated with a layer of sputtered Au−Pd. Quantitative analysis of SEM images was performed to estimate the fiber diameters, using image process and analysis in Java (Image-J, NIH) software. For light microscopic observation, electrospun nanofibers were stained with 100 μL Alizarin Red S solutions and rinsed with DI water prior to observation.

Hydrogen peroxide production was analyzed by measuring the amount of calcium hydroxide released in DI water. Specifically, a nanofiber mesh with lateral dimensions of ~1 in ×1 in was weighed, then immersed in 1 mL of DI water, and incubated at 37 °C in an orbital shaking incubator (New Brunswick Scientific, NJ) at 120 rpm. The resulting solution was sampled at time points of 24, 48, and 72 h, and the calcium hydroxide concentration was measured by a modified Alizarin Red S assay (30). Briefly, 100 μL of 2 mg/mL Alizarin Red S solution (pH 4.1) was added to the 1 mL solution in a 1.5 mL centrifuge tube, and a red precipitate formed immediately when the regent reacted with calcium ions within the solution. The red precipitate was concentrated by ultrahigh centrifuge at 4 °C and 13.2 krpm for 15 min. The supernatant was removed, the precipitate was rinsed with DI water, and it was then recentrifuged. This cleaning process was repeated 3 times. To quantify the amount of calcium peroxide released, we then solubilized the red calcium precipitate in 10% (w/v) cetylpyridinium chloride (Sigma), and the optical density of the solution was measured at 562 nm with a calibrated microplate reader (BioTek). The amount of hydrogen peroxide generated could be estimated as the equivalent mole of the calcium hydroxide and then normalized by the fiber weight.

Antimicrobial Evaluation. *E. coli* (ATCC 8739) and *S. epidermidis* (ATCC 12228) were cultured in sterilized Lysogeny broth (LB) medium and Tryptic Soy Broth medium (TSB), respectively, and then incubated overnight at 37 °C with a shaking incubator. Bacterial suspensions containing from 1 × 10^7 to 1 × 10^8 colony forming units (CFU) were employed for evaluation. Specifically, nanofiber-coated silicon wafers were placed in flat-bottomed 24-well tissue culture plates, and each

wafer was inoculated with 5 μL of the bacterial suspension. After 10 min, 2 mL of culture medium was then added to each well. The plates were kept at 37 °C for either 6 or 24 h. After incubation, the samples were rinsed with phosphate buffered saline (PBS) and moved to a new 24-well plate containing 1 mL of PBS in each well. The MTS-PMS colorimetric assay was conducted by adding 3-(4,5-dimethylthiazol-2-yl)-5-(3-carboxymethoxyphenyl)-2-(4-sulfophenyl)-2H-tetrazolium and phenylmethasulfazone (MTS-PMS) reagents (40 μL) (Promega) to each well followed by incubation for an additional 1 h. Besides the oxygen-generating nanofibers, unmodified silicon wafer and silicon wafer modified by a coating of PCL fibers were used as negative controls in these tests. The number of viable bacteria was determined colorimetrically by measuring the formazan concentration, the soluble reduction product of MTS-PMS, at 490 nm using a microplate reader (Bio-Tek Instruments).

To perform a modified Kirby–Bauer type test, a nanofiber mesh sample was cut into equal-sized round pieces (1 cm in diameter), and each piece was placed on the *E. coli* grown on an LB agar plate. After overnight incubation at 37 °C, the zone of inhibition was measured.

Human Osteoblast Response. Human osteoblast cells (hFOB 1.19, ATCC) were used as model tissue cells for evaluation of the cellular responses to the nanofibers. Cells were cultured in a 1:1 mixture of Ham's F12 medium (GIBCO) and Dulbeccco's Modified Eagle Medium-Low Glucose (DMEM-LG; Sigma) supplemented with 1% penicillin-streptomycin (Invitrogen) and 10% fetal bovine serum (FBS) (Invitrogen). During culture, cells were maintained in a humidified atmosphere of 5% CO_2 at 37 °C.

These cell experiments were conducted in 96-well plates with one sample in each well. Prior to an experiment, nanofiber meshes were equilibrated in fresh medium for half an hour in order to facilitate cell adhesion to them. After that, 40 μL of human osteoblast cell suspension was placed in each well at a cell seeding density at 1 × 10^5cells/well. After 2 h incubation, 200 μL of medium was added to each well to maintain the cell culture on the scaffolds. The medium was changed after 2 days.

Cell viability after 1 and 4 days was analyzed by performing a cell proliferation assay. After incubation, cell numbers were determined using the CellTiter 96 aqueous non-radioactive cell proliferation assay (Promega) according to the protocol provided by the manufacturer. The CellTiter 96 aqueous assay is composed of solutions of a tetrazolium compound (3-(4,5-dimethylthiazol-2-yl)-5-(3-carboxymethoxyphenyl)-2-(4-sulfophenyl)-2H-tetrazolium, inner salt; MTS) and an electron coupling reagent (phenazine methosulfate; PMS). MTS is bioreduced by metabolically active cells into a formazan product that is soluble in tissue culture medium. The absorbance of the formazan at 490 nm, which can be measured directly from 96 well assay plates with a micro plate reader (BioTek), is directly proportional to the number of living cells in culture. Therefore, the absorbance at 490 nm was used to quantify cell proliferation on the nanofibers.

To study possible changes in cell morphology at the end of the incubation period, we fixed cells in 4% paraformaldehyde and stained with FITC-phalloidin (Molecular Probes) for confocal laser scanning microscopy (CLSM). Images were scanned using a LSM 700 flexible confocal microscope (CLSM) through 20× objectives.

Statistical Analyses. All quantitative data were reported as the mean ± the standard deviation. Statistical differences between each sample were determined by performing a one-way ANOVA test. The multiple pairwise comparisons were performed using a Bonferroni post hoc analysis at 95% confidence.

RESULTS AND DISCUSSION

Nanofiber Characterization. As illustrated in Figure 1, Alizarin red S staining shows that calcium peroxide was

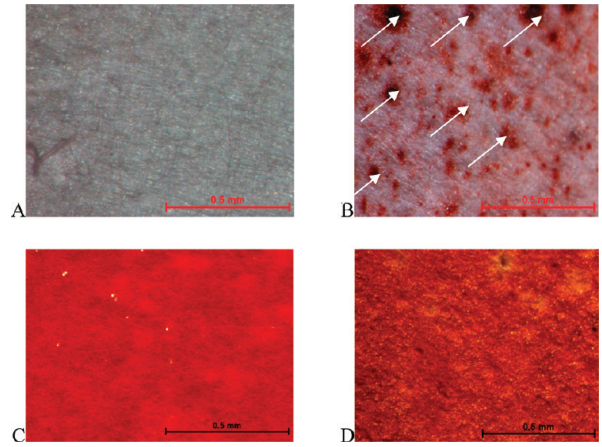

FIGURE 1. Calcium staining of four groups of PCL-based nanofibers: (A) 0% CP/PCL; (B) 1% CP/PCL; (C) 5% CP/PCL; and (D) 10% CP/PCL. (Arrows in B show calcium peroxide dispersed within nanofibers, whereas in C and D, too much calcium peroxide was incorporated, forming a coating layer on the surface of nanofibers.)

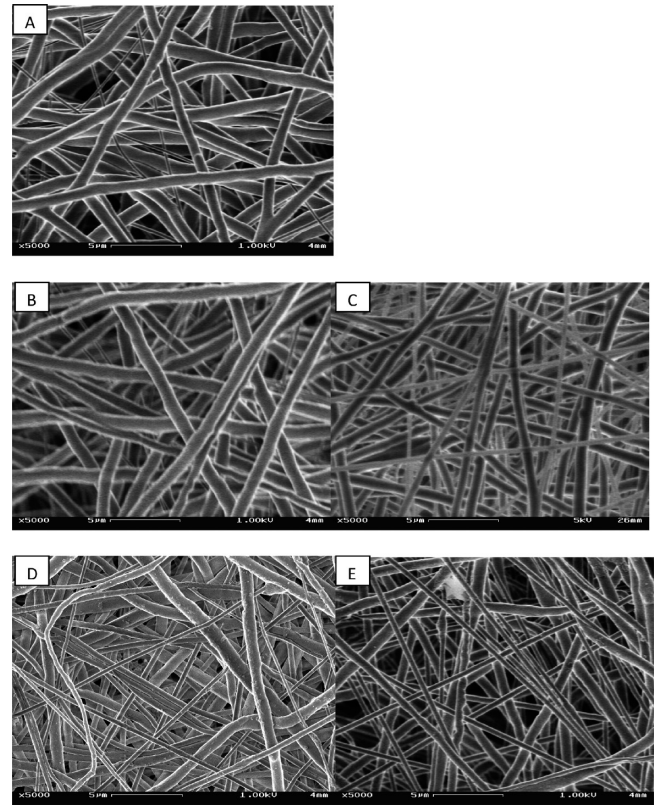

FIGURE 2. Scanning electron micrographs of electrospun nanofibers with compositions of: (A) PCL; (B) PCL/CP 10%; (C) PCL/CP/AC 10%; (D) DI water-treated PCL/CP 10%; and (E) DI water-treated PCL/CP/AC 10%.

successfully incorporated in the PCL nanofibers. SEM images (Figure 2) showed the morphology of calcium peroxide loaded nanofibers. Incorporation of calcium peroxide and ascorbic acid did not change the fiber diameter significantly in comparison with the PCL fibers (Table 2). However, after the calcium peroxide and ascorbic acid were leached out by the DI water, the majority of the DI water-treated fibers became thinner (Figure 2D,E). The fiber diameter dropped from an average of 800 nm to an average of 400 nm (Table 2) after DI water treatment. It was also found that the

Table 2. Characterization of Oxygen-Generating Nanofibers (* statistically significant smaller fiber diameter of DI water-treated nanofibers than original fibers, $n = 5$)

	original fibers			DI water- treated	
	PCL	PCL 10%CP	PCL 10%CP, 10%AC	PCL 10%CP	PCL 10%CP, 10%AC
diameter (nm)	807	875	759	401*	409*
standard deviation (nm)	100	189	95	202	174

integrity of the fiber mesh was not affected after the salts were leached out in reaction with water (Figure 2). These results suggest that most of the calcium peroxide loaded might be located on the surface of the nanofibers.

The results of the release study (Figure 3) demonstrate that a burst release of calcium peroxide occurred at day 1. This burst-release behavior again suggests that most of the calcium peroxide is located on or near the nanofiber surfaces. Furthermore the incorporation of ascorbic acid also enhances the burst release of the calcium peroxide. We speculate that this is because dissolution of ascorbic acid would create greater porosity in the nanofibers, thus exposing even more surface for calcium peroxide release.

Antimicrobial Activity of Fibers. The antimicrobial activity of oxygen generating nanofibers was evaluated using the modified Kirby-Bauer test and MTS-PMS assay. Gram-negative (*E. coli*) and Gram-positive (*S. epidermidis*) bacterial strains were chosen, as causative organisms of many device-related infections. The quantitative evaluation of antimicrobial activity of the oxygen-generating fibers against *S. epidermidis* and *E. coli* was examined through an MTS-PMS assay based on the reduction of MTS, in the presence of PMS as an electron-coupling agent. The results shown in Figure 4 demonstrate that the incorporation of calcium peroxide into the PCL nanofibers could suppress bacterial growth in a dose-dependent manner. The incorporation of 10% calcium peroxide to the PCL nanofibers reduced *E. coli* growth up to 95%, and reduced *S. epidermidis* growth up to 90% at 24 h. The contact biocidal property of PCL-CP (10%) nanofiber was also investigated by using a modified Kirby-Bauer test. PCL-CP (10%) nanofiber was placed on a lawn of *E. coli*

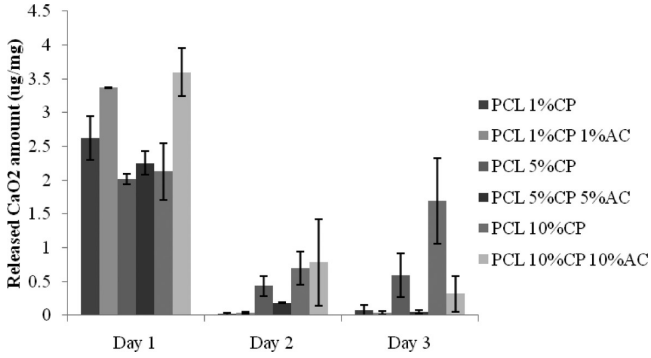

FIGURE 3. Daily release of calcium peroxide from the nanofibers (normalized by the weight of nanofiber). Error bar denotes standard deviation (SD); three samples were tested for the experiment and all data points plotted as mean values ± SD.

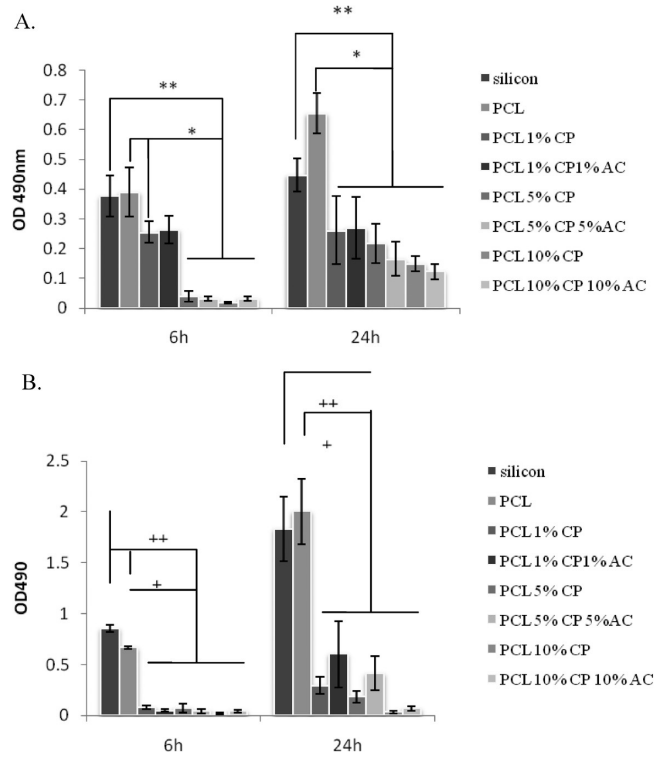

FIGURE 4. (A) *S. epidermidis* and (B) *E. coli* growth on different groups of samples at 37 °C for 6 h and 24 h. Data represent mean (± SD) of 4 replicate wells. * indicates a statistically significant ($p < 0.05$) higher number of *S. epidermidis* on PCL nanofiber mesh than on the oxygen-generating nanofibers after 6 h and 24 h incubation except group PCL 1%CP and 1% AC at 6 h; ** indicates a statistically significant higher number of *S. epidermidis* on silicon than on the oxygen-generating nanofibers after 6 h and 24 h incubation except group PCL 1%CP and PCL 1%CP 1% AC at 6 h; + indicates a statistically significant higher number of *E. coli* on the PCL nanofiber mesh than on the oxygen-generating nanofibers after 6 h and 24 h incubation; ++ indicates a statistically significant higher number of *E. coli* on silicon than on the oxygen-generating nanofibers after 6 h and 24 h incubation.

in an agar plate. A clear zone of inhibition around the nanofiber after 24 h incubation (Figure 5) was observed in comparison with the PCL nanofiber control group, which does not have any inhibitory effect on the growth of *E.coli*.

These results show that the burst release of calcium peroxide effectively inhibits bacterial growth with two reaction products acting as biocides. The significant reduction of bacterial growth will decrease the possibility of biofilm development. Such a release profile is consistent with a strategy to kill pre-operatively introduced organisms and thus reduce the probability that bacteria will colonize an implant surface. An initial burst release in local delivery of antimicrobial agents is highly desirable for most infection cases, and many studies have proved its efficacy (31, 32). Furthermore, this strategy can also target the complications of current antibiotic-releasing bone cements, where the long-term exposure to low doses of antibiotics released from bone cements can lead to antibiotic resistance (33).

Cellular Response of Antimicrobial Nanofibers. The results of our cell-viability study are presented in Figure 6. These show that calcium peroxide has some cytotoxity to the osteoblasts at day 1 as a result of initial burst release of biocides. However, at day 4, there was no significant

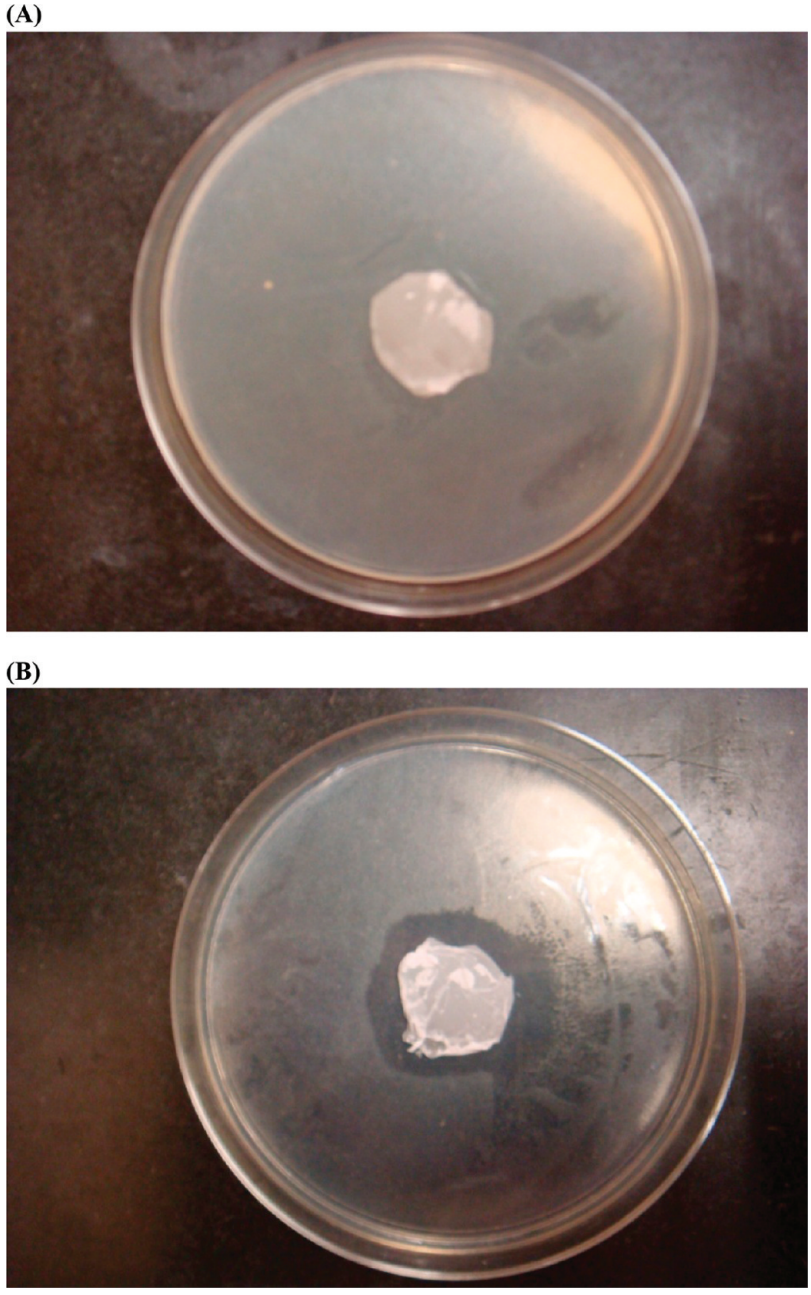

FIGURE 5. Inhibition zones observed by a modified Kirby–Bauer test after 24 h on agar incubated with *E. coli* around: (A) PCL nanofiber mesh; and (B) PCL/10% CP nanofiber mesh.

difference in cell numbers between the PCL-CP fibers and the unloaded PCL fiber control after the medium was replaced at day 2. These results demonstrate that the cytotoxicity of the oxygen-generating fibers was significantly reduced after longer-term incubation. We attribute this reduced cytotoxicity to the fact that the release of hydrogen peroxide decreases significantly after the initial one-day burst (Figure 3).

Many previous studies have demonstrated the cytotoxity of H_2O_2 to osteoblast cells in both a dose-dependent and time-dependent manner. The killing of cells is mediated by the generation of reactive oxygen species (ROS) (34). It has been shown that both the cell numbers and the expressed alkaline phosphatase activity as well as the formation of mineralized matrix are significantly reduced by H_2O_2 (35, 36). These adverse effects can be counteracted by the addition, for example, of purines (13), biochanin A (37), 2, 6-diisopropylphenol (38), or pyruvates (39), which either act as antioxidants or contribute to blocking the necrotic or apoptotic cell pathways. In our study, we used ascorbic acid to alleviate the adverse effect on the osteoblast cells. As shown in Figure 6, cell numbers on samples with the addition of ascorbic acid are significantly higher than those without ascorbic acid.

Figure 7 presents fluorescence images depicting cell morphology after F-actin staining by the FITC-Phalloidin. At day 1, when the osteoblasts encountered the released hydrogen peroxide, the osteoblasts shrink, forming an unhealthy spherical shape (Figure 7A–C). The incorporation of ascorbic acid was able to protect the cells to some extent

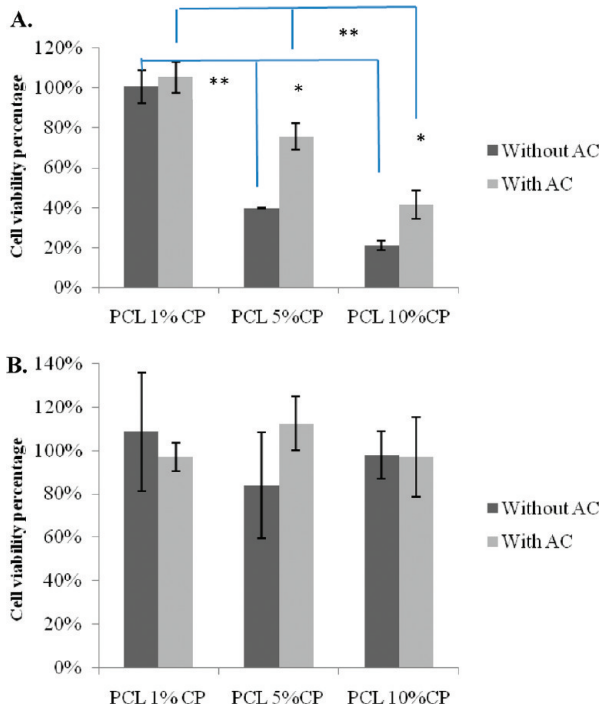

FIGURE 6. Cell viability on the oxygen-generating fibers. Human osteoblast cells were cultured on the fibers and an MTS−PMS assay was conducted at (A) day 1 and (B) day 4. The viability was denoted as the percentage of viable cells on the oxygen generating fibers relative that on the PCL fibers. Data represent the mean (± SD) of 4 replicate wells. *, A significantly higher cell viability percentage for oxygen generating nanofibers with acorbic acid than groups without at day 1; **, a significant reduction of cell viability percentage for oxygen generating nanofibers with the increasing ratio of calcium peroxide at day 1.

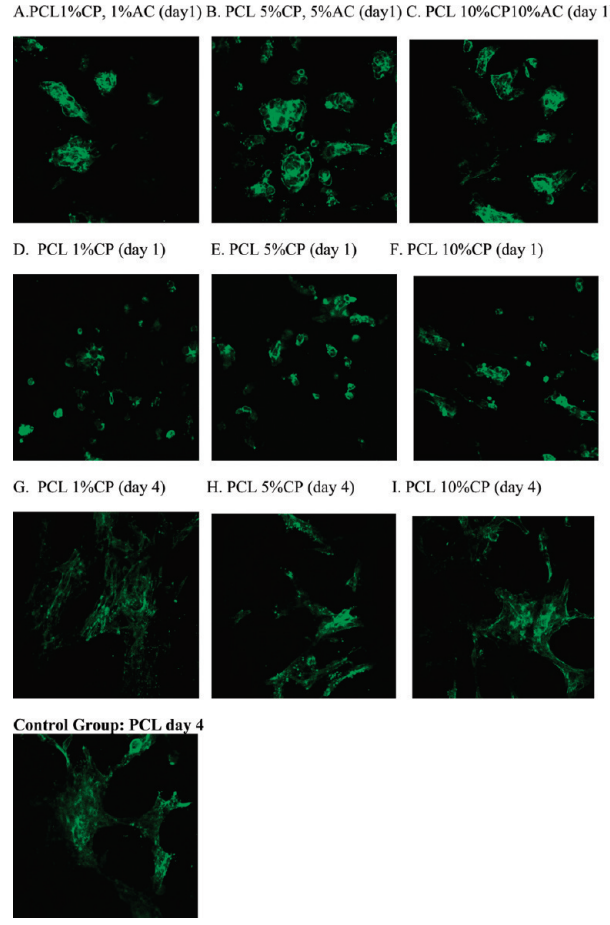

FIGURE 7. Confocal microscopic images of cells cultured on the oxygen-generating fibers at (A−F) day 1 and (G−I) day 4 (magnification: 200).

as manifested by the fact that the cells could still keep a spindle shape (Figure 7A). However, at day 4, after the medium was changed at day 2, the osteoblasts recovered a healthy status (Figures 7 G − 7I) where they spread on the nanofiber mesh. The early damage to these cells was therefore transient, and these results suggest that there would be no long-term harm to tissue development if an oxygen-generating fiber matte was used as an implant-coating material. Therefore fast release pattern of this oxygen generating nanofibers led to a low level of peroxide release in the latter stage. This allowed the minimum negative effect of the system to bone healing which existed in the slow release system. Several in vitro and in vivo studies and first clinical cases has proved that locally delivered antibiotics from implants with an initial burst release at high concentration could be an effective supplement to reduce the infection rate during orthopedic surgery (12). Furthermore, the antimicrobial capacity of calcium peroxide loaded in the nanofibers could be easily modulated by adjusting the ratio of calcium peroxide to the polymer based on different requirements. However, the temporary side effect of hydrogen peroxide should be considered and therefore the ratio should be optimized within a safety range in the future work. Significant difference of inhibition effect on two types of bacteria has not been observed in the 6 h and 24 h antimicrobial study. However it is possible that ascorbic acid could also provide protection for the bacteria. The different interaction mechanism of cells and bacterial to antibacterial reagent could explain the difference response of cells and bacteria. It is obvious that more study need to be performed in order to elaborate this phenomena.

Calcium peroxide has been applied as an oxygen generating agent for enhanced tissue survival with slow sustained release from a 3D tissue-engineered constructs (40), whereas in our study, calcium peroxide was employed as biocider agent with burst release from nanofibers. To our knowledge, this is the first time that calcium peroxide has been incorporated into nanofibers to act as an antimicrobial agent. The strategy of applying this type of antimicrobial nanofiber to prevent the biofilm formation is to destroy most bacteria in the early stage of implantation by using cost-effective materials. Moreover, the hydrogen peroxide could be quickly eliminated after interacting to the implantation surface, thus no long-term cytotoxicity issue would be caused. Specifically for tissue engineering application, materials used within this system are biodegradable so that no further surgical removal was needed for this application. Nanofiber meshes used for bone repair would enhance bone healing and promote bone integration with the implanted device due to their biomimetic structures (41).

CONCLUSION

We have demonstrated that calcium peroxide can be incorporated into PCL nanofibers and generate H_2O_2 and calcium hydroxide when exposed to water. The initial burst release of H_2O_2 and calcium hydroxide effectively suppresses the growth of Gram-positive (*S. epidermidis*) as well as of Gram-negative bacteria (*E. coli)*. Although a certain level of cytotoxicity to human osteoblast cells was observed during the burst release period, cells recovered when the concentration of H_2O_2 was lowered after 4 days of culture indicating that there is no long-term toxicity of this type of material. These results suggest that such nanofibers could be a good candidate material to coat an orthopedic implant in order to promote bone ingrowth, while simultaneously reducing the threat of bacterial colonization and subsequent chronic infection of surrounding tissue.

Acknowledgment. The authors are grateful for the help of Wei Liu and Ami Shah during the preliminary studies in this project. The authors also thank Qichen Wang for her valuable discussion regarding biofilm prevention strategies. This research project has been partially supported by the National Science Foundation through Grant CBET-0708379.

REFERENCES AND NOTES

(1) Manangan, L. P.; Pearson, M. L.; Tokars, J. I.; Miller, E; Jarvis, W. R. *Emerging Infect. Dis.* **2002**, *8*, 233–236.
(2) Hall-Stoodley, L; Costerton, J. W.; Stoodley, P. *Nat. Rev. Microbiol.* **2004**, *2*, 95–108.
(3) Vu, B; Chen, M; Crawford, R. J.; Ivanova, E. P. *Molecules* **2009**, *14*, 2535–2554.
(4) Costerton, J. W.; Stewart, P. S.; Greenberg, E. P. *Science* **1999**, *284*, 1318–1322.
(5) Darouiche, R. O. *New Engl. J. Med.* **2004**, *350*, 1422–1429.
(6) Pavithra, D.; Doble, M. *Biomed. Mater.* **2008**, *3*, 034003.
(7) Campoccia, D; Montanaro, L; Arciola, C. R. *Biomaterials* **2006**, *27*, 2331–2339.
(8) Arciola, C. R.; Alvi, F. I.; An, Y. H.; Campoccia, D.; Montanaro, L. *Int. J. Artif. Organs* **2005**, *28*, 1119–1125.
(9) Hedrick, T. L.; Adams, J. D.; Sawyer, R. G. *J. Long-Term Eff. Med. Implants* **2006**, *16*, 83–99.
(10) Khoo, X.; Hamilton, P.; O'Toole, G. A.; Snyder, B. D.; Kenan, D. J.; Grinstaff, M. W. *J. Am. Chem. Soc.* **2009**, *131*, 10992–7.
(11) Gottenbos, B.; van der Mei, H. C.; Klatter, F.; Grijpma, D. W.; Feijen, J.; Nieuwenhuis, P.; Busscher, H. J. *Biomaterials* **2003**, *24*, 2707–2710.
(12) Von Eiff, C.; Kohnen, W.; Becker, K.; Jansen, B. *Int. J. Artif. Organs* **2005**, *28*, 1146–1156.
(13) Busscher, H. J.; Ploeg, R. J.; Van der Mei, H. C. *Biomaterials* **2009**, *30*, 4247–4248.
(14) Koort, J. K.; Mäkinen, T. J.; Suokas, E.; Veiranto, M.; Jalava, J.; Knuuti, J.; Törmälä, P.; Aro, H. T. *Antimicrob. Agents Chemother.* **2005**, *49*, 1502–1508.
(15) Hetrick, E. M.; Shin, J. H.; Paul, H. S.; Schoenfisch, M. H. *Biomaterials* **2009**, *30*, 2782–2789.
(16) Buzoglu, H. D.; Gümüsderelioğlu, M.; Rotstein, I. *Am. J. Dent* **2009**, *22*, 223–227.
(17) Monteiro, D. R.; Gorup, L. F.; Takamiya, A. S.; Ruvollo-Filho, A. C.; de Camargo, E. R.; Barbosa, D. B. *Int. J. Antimicrob. Agents.* **2009**, *34*, 103–110.
(18) Jakubovics, N. S.; Gill, S. R.; Vickerman, M. M.; Kolenbrander, P. E. *FEMS Microbiol. Ecol.* **2008**, *66*, 637–644.
(19) Presterl, E.; Suchomel, M.; Eder, M.; Reichmann, S.; Lassnigg, A.; Graninger, W.; Rotter, M. *J. Antimicrob. Chemother.* **2007**, *60*, 417–420.
(20) Szymañska, J. *Ann. Agric. Environ. Med.* **2006**, *13*, 313–317.
(21) Miller, R. A.; Britigan, B. E. *Clin. Microbiol. Rev.* **1997**, *10*, 1–18.
(22) Glynn, A. A.; O'Donnell, S. T.; Molony, D. C.; Sheehan, E.; McCormack, D. J.; O'Gara, J. P. *J. Orthop. Res.* **2009**, *27*, 627–630.
(23) Baldeck, J. D.; Marquis, R. E. *Can. J. Microbiol.* **2008**, *54*, 868–875.
(24) Richards, G.; Harris, L. G.; Schneider, E.; Haas, N. *Injury* **2006**, *37*, S113–116.
(25) Kristensen, J. B.; Olsen, S. M.; Laursen, B. S.; Kragh, K. M.; Poulsen, C. H.; Besenbacher, F.; Meyer, R. L. *Biofouling* **2010**, *26*, 141–153.
(26) Chai, W. L.; Hamimah, H.; Cheng, S. C.; Sallam, A. A.; Abdullah, M. J. *Oral. Sci.* **2007**, *49*, 161–166.
(27) Desai, S.; Chandler, N. J. *Endodontics* **2009**, *35*, 475–480.
(28) Noetzel, J.; Nonhoff, J.; Bitter, K.; Wagner, J.; Neumann, K.; Kielbassa, A. M. *Am. J. Dent.* **2009**, *22*, 14–18.
(29) Duarte, T. L.; Lunec, J. *Free Radical Res.* **2005**, *39*, 671–686.
(30) Wang, J.; Valmikinathan, C. M.; Liu, W.; Laurencin, C. T.; Yu, X. J. *Biomed. Mater. Res., A* **2010**, *93*, 753–762.
(31) Shukla, A.; Fleming, K. E.; Chuang, H. F.; Chau, T. M.; Loose, C. R.; Stephanopoulos, G. N.; Hammond, P. T. *Biomaterials* **2010**, *31*, 2348–2357.
(32) Stallmann, H. P.; Faber, C.; Slotema, E. T.; Lyaruu, D.M.; L, A.L.; Bronckers, J. J.; Amerongen, A. V. N.; Wuisman, Paul I. J. M. *J. Antimicrob. Chemother.* **2003**, *52*, 853–855.
(33) Wencewicz, T. A.; Möllmann, U.; Long, T. E.; Miller, M. J. *Biometals* **2009**, *22*, 633–648.
(34) Chae, H. J.; Kang, J. S.; Han, J. I.; Bang, B. G.; Chae, S. W.; Kim, K. W.; Kim, H. M.; Kim, H. R. *Immunopharmacol. Immunotoxicol.* **2000**, *22*, 317–337.
(35) Fatokun, A. A.; Stone, T. W.; Smith, R. A. *Bone* **2006**, *39*, 542–551.
(36) Lee, D. H.; Lim, B. S.; Lee, Y. K.; Yang, H. C. *Cell Biol. Toxicol* **2006**, *22*, 39–46.
(37) Lee, K. H.; Choi, E. M. *Biol. Pharm. Bull.* **2005**, *28*, 1948–1953.
(38) Chen, R. M.; Wu, G. J.; Chang, H. C.; Chen, J. T.; Chen, T. F.; Lin, Y. L.; Chen, T. L. *Ann. N.Y. Acad. Sci.* **2005**, *1042*, 448–459.
(39) Hinoi, E.; Takarada, T.; Tsuchihashi, Y.; Fujimori, S.; Moriguchi, N.; Wang, L.; Uno, K.; Yoneda, Y. *Mol. Pharmacol.* **2006**, *70*, 925–935.
(40) Oh, S. H.; Ward, C. L.; Atala, A.; Yoo, J. J.; Harrison, B. S. *Biomaterials* **2009**, *30*, 757–762.
(41) Sargeant, T. D.; Guler, M. O.; Oppenheimer, S. M.; Mata, A.; Satcher, R. L.; Dunand, D. C.; Stupp, S. I. *Biomaterials* **2008**, *29*, 161–171.

AM100862H